



HAL
open science

Diffusion tensor imaging and gray matter volumetry to evaluate cerebral remodeling processes after a pure motor stroke: a longitudinal study

Isabelle Loubinoux, Marie Lafuma, Julien Rigal, Nina Colitti, Jean-François Albucher, Nicolas Raposo, Mélanie Planton, Jean-Marc Olivot, François Chollet

► To cite this version:

Isabelle Loubinoux, Marie Lafuma, Julien Rigal, Nina Colitti, Jean-François Albucher, et al.. Diffusion tensor imaging and gray matter volumetry to evaluate cerebral remodeling processes after a pure motor stroke: a longitudinal study. *Journal of Neurology*, 2024, 10.1007/s00415-024-12648-y . hal-04711991

HAL Id: hal-04711991

<https://hal.science/hal-04711991v1>

Submitted on 27 Sep 2024

HAL is a multi-disciplinary open access archive for the deposit and dissemination of scientific research documents, whether they are published or not. The documents may come from teaching and research institutions in France or abroad, or from public or private research centers.

L'archive ouverte pluridisciplinaire **HAL**, est destinée au dépôt et à la diffusion de documents scientifiques de niveau recherche, publiés ou non, émanant des établissements d'enseignement et de recherche français ou étrangers, des laboratoires publics ou privés.



Distributed under a Creative Commons Attribution 4.0 International License



Diffusion tensor imaging and gray matter volumetry to evaluate cerebral remodeling processes after a pure motor stroke: a longitudinal study

Isabelle Loubinoux¹ · Marie Lafuma^{1,2} · Julien Rigal^{1,2} · Nina Colitti¹ · Jean-François Albucher^{1,2} · Nicolas Raposo^{1,2} · Mélanie Planton^{1,2} · Jean-Marc Olivot^{1,2} · François Chollet^{1,2}

Received: 13 March 2024 / Revised: 5 July 2024 / Accepted: 17 August 2024

© The Author(s) 2024

Abstract

Background and objectives Clinical factors are not sufficient to fix a prognosis of recovery after stroke. Pyramidal tract or alternate motor fiber (aMF: reticulo-, rubrospinal pathways and transcallosal fibers) integrity and remodeling processes assessable by diffusion tensor MRI (DTI) and voxel-based morphometry (VBM) may be of interest. The primary objective was to study longitudinal cortical brain changes using VBM and longitudinal corticospinal tract changes using DTI during the first 4 months after lacunar cerebral infarction. The second objective was to determine which changes were correlated to clinical improvement.

Methods Twenty-one patients with deep brain ischemic infarct with pure motor deficit (NIHSS score ≥ 2) were recruited at Purpan Hospital and included. Motor deficit was measured [Nine peg hole test (NPHT), dynamometer (DYN), Hand-Tapping Test (HTT)], and a 3T MRI scan (VBM and DTI) was performed during the acute and subacute phases.

Results White matter changes: corticospinal fractional anisotropy (FA_{CST}) was significantly reduced at follow-up (approximately 4 months) on the lesion side. FA_r (FA ratio in affected/unaffected hemispheres) in the corona radiata was correlated to the motor performance at the NPHT, DYN, and HTT at follow-up. The presence of aMFs was not associated with the extent of recovery. Grey matter changes: VBM showed significant increased cortical thickness in the ipsilesional premotor cortex at follow-up. VBM changes in the anterior cingulum positively correlated with improvement in motor measures between baseline and follow-up.

Discussion To our knowledge, this study is original because is a longitudinal study combining VBM and DTI during the first 4 months after stroke in a series of patients selected on pure motor deficit. Our data would suggest that good recovery relies on spared CST fibers, probably from the premotor cortex, rather than on the aMF in this group with mild motor deficit. The present study suggests that VBM and FA_{CST} could provide reliable biomarkers of post-stroke atrophy, reorganization, plasticity and recovery.

ClinicalTrials.gov Identifier NCT01862172, registered May 24, 2013

Keywords DTI MRI · Recovery of function · Diffusion tractography · Atrophy · Brain regeneration

Introduction

As the leading cause of acquired adult disability, the third leading cause of death, stroke is a public health problem. Acute-phase therapeutic strategies such as thrombolysis and

thrombectomy have improved functional prognosis. However, only 15% of stroke patients can benefit from these revascularization treatments and more than half of these treated patients have a Rankin score > 2 after 3 months [1]. Thus, motor deficit is the most common persistent clinical disability and affects approximately 80% of patients. At 6 months, 50% of patients over 65 years old have a persistent motor deficit [2]. The challenge is to better understand the mechanisms of neurological recovery and cerebral reorganization post-stroke. It is not known at this time whether the improvement in motor impairment is best explained by

✉ Isabelle Loubinoux
isabelle.loubinoux@inserm.fr

¹ Toulouse NeuroImaging Center (ToNIC), Toulouse, France

² Neurology Department, Toulouse, France

changes in structural connections or by functional connections of the motor system. A better knowledge of the mechanisms of cerebral plasticity can lead, in a second step, to therapeutic intervention studies. Reorganization and plastic changes underlying recovery also depend heavily on the phases of recovery [3] and homogeneously recruited populations will lead to more accurate findings. The study of focal lacunar infarcts is a first step towards understanding these plastic changes.

DTI is a magnetic resonance imaging technique for *in vivo* quantification of microstructural damage to white matter tracts following stroke. It assesses fractional anisotropy (FA) which is an index of Wallerian degeneration [4]. FA reflects the total amount of diffusion and is quite sensitive to a number of tissue properties, such as axonal ordering, axonal density, and degree of myelination, without being very specific to any one of them. It combines the contributions from the different sub-compartments of white matter into a single measure. Multiple prior studies on large infarcts have demonstrated a correlation between FA of the corticospinal tract (CST) and motor performance in stroke patients [5–7], including some longitudinal studies [7–9]. Other studies explore premotor or prefrontal pathways [10–14]. Studies more focused on lacunar infarcts corroborated these findings [10–12].

Reorganization and recovery probably depend also on remodeling in the cortical regions and indeed functional connectivity between cortical and subcortical networks. Voxel-based morphometry (VBM) has been developed by Ashburner and Friston in 2000 [15]. It evaluates brain structural abnormalities, including changes in gray matter, on T1-weighted MRI images. These structural changes are evaluated by comparing the assessment of local gray matter concentration between each voxel of images of two groups of subjects or on subjects explored longitudinally. Dang et al. [16], in a longitudinal MR study proved that changes in gray matter volumes, especially in specific motor-relevant brain regions occurring distal to the primary subcortical cerebral infarct, were associated with functional recovery after subcortical infarct. Furthermore, combining diffusion tensor imaging and VBM can better characterize natural evolution of cerebral remodeling processes after motor deficit.

To our knowledge, only three studies [17–19] have assessed the correlation between motor recovery using DTI and VBM together. These three studies included between 17 and 31 patients with various post-stroke follow-up times (between 3 months and several years) and no longitudinal follow-up. Besides, one study included ischemic and hemorrhagic strokes [19].

Here, we measure the longitudinal changes in FA_{CST} with DTI and remodeling in cortical regions with VBM and their relationship with motor recovery in a longitudinal study of post-stroke patients. Study of the corticospinal tract (FA_{CST} ,

MD, AD, RD, mean, axial and radial diffusivities, respectively) was restricted to the tract emanating from the primary motor cortex. We hypothesized that corticospinal atrophy assessed by DTI and increased cortical thickness assessed by VBM would correlate with clinical recovery.

Methods

Subjects

Between February 2013 and July 2014, patients were recruited in this longitudinal study within the first 10 days after stroke via the stroke unit of Toulouse Hospital. Twenty-one patients (aged 18–90) with a pure motor deficit (NIHSS > 2) showed a first subcortical infarct proven by MRI. Cortical localization of the ischemic stroke, multiple stroke localizations, MRI contra-indication, coma, and history of psychiatric disease were exclusion criteria. Motor deficit was measured in the acute (first 10 days, baseline) phase and at follow-up (approximately 4 months after stroke onset) including the NIHSS, the Nine Peg Hole test (NPHT), the Hand-Tapping Test (HHT) and the dynamometer (DYN). This study was approved local Ethics Committee (Comité de Protection des Personnes Sud-Ouest et Outre-Mer I, n°12 483 03) and ANSM (Agence Nationale de Sécurité du Médicament et des produits de la santé, n°B121418-31) (ClinicalTrials.gov Identifier: NCT01862172, registered May 24, 2013).

Imaging data acquisition

Imaging data were acquired at the same time points as clinical examination (first 10 days and approximately 4 months after stroke). A 3T Philips ACHIEVA MRI scanner and a 32-channel coil were used to acquire both diffusion-weighted imaging and high-resolution T1-weighted anatomic images. Fluid-attenuated inversion recovery (3D FLAIR; TR 8000 ms; TE 337 ms; inversion time 2400 ms; matrix $240 \times 240 \times 170$; field of view (FOV) $240 \times 240 \times 170$; voxel size $1 \times 1 \times 1$, sagittal slices, duration time 6.16 min. For diffusion tensor imaging, 62 axial slices were obtained covering the whole brain with gradients ($b = 1000 \text{ s/mm}^2$) applied along 32 non-collinear directions with the following parameters: repetition time (TR): 7 s, echo time (TE) = 73 ms, FOV $224 \times 224 \times 124$; voxel size = $2 \times 2 \times 2$ mm, one B0, acquisition time: 9 min. Then, T1-weighted 3D magnetization prepared rapid gradient echo images (TR = 8,1 ms; TE = 3,7 ms; FOV = $220 \times 132 \times 170$, voxel size = $1 \times 1 \times 1$ mm) were also acquired in 4.20 min. To improve signal to noise ratio and reduced variability in acquisition [20], two acquisitions were made. Images of patient with a lesion in the right hemisphere

were flipped, relative to the mid-sagittal plane, to the left hemisphere.

Data processing

DTI

Diffusion-weighted images were analyzed using the diffusion spectrum imaging (DSI Studio) software (<http://dsi-studio.labsolver.org>). All data sets were corrected for eddy currents and head motion. With white matter Human Connectome Project atlas (HCP842 atlas), fiber tracking was based on an automatic fiber tracking function and a deterministic fiber tracking algorithm using a track recognition based on the tractography atlas [21]. The normalized diffusion images were superimposed on the MNI template for each subject to check normalization. Voxels at zero intensity were automatically eliminated. Fiber tracking was done by assigning regions as seeding region: primary motor cortex, ROIs: CR_{sup} (superior corona radiata), PLIC (posterior limb of the internal capsule), cerebral peduncle, and ending region: pontine crossing tract, and corticospinal tract. It was followed by the calculation of FA, MD, AD, and RD. The FA threshold was set to 0.2 and the angular threshold between 45 and 65°. DTI parameters were extracted for the corticospinal tract generated by the fiber tracking and the FA for three regions of interest (ROI) of the corticospinal tract: PLIC, corona radiata (CR) and pons. When the fibers generated by CST exploration drifted outside the true CST, correspondence with the corpus callosum, rubro- and reticulospinal (supplementary Fig. 1) tracts was also explored using the respective templates.

VBM

For VBM, we used the statistical Parametric toolbox (SPM 12) implemented on MATLAB and CAT12 (<https://neurojena.github.io/cat/>). VBM involves voxel-wise comparisons of local gray matter density or volume. The two T1 acquisitions acquired the same day were averaged (meanT1). For patients who had a lesion in the right hemisphere, their images were flipped, across the mid-sagittal plane, to the left hemisphere, for comparison purposes. Stroke lesions were masked out via manual tracing using MRICron software and were not considered during the registration process. To do so, for each patient, we created a binary lesion mask depicting the lesion boundaries, using MRICron software [22] (<http://www.sph.sc.edu/comd/rorden/mricron/>). The lesion was first identified using the T1 sequence, after which the lesion volume of interest (VOI) was drawn on each affected slice. The VOI was then smoothed using a 4-mm FWHM Gaussian filter with a 0.1% threshold [23]. A lesion-masked T1 was then created by merging the specific

patient's T1 and lesion VOI, using the 'Imcalc' function of SPM12 Toolbox (Wellcome Centre for Human Neuroimaging, London, UK; <http://www.fil.ion.ucl.ac.uk/spm/>) with the formula $i1 * .i2$. CAT12 deals with lesions that have to be set to "0" in the images using the stroke lesion correction (SLC). These lesion areas are not used for segmentation or spatial registration, thus these preprocessing steps should be almost unaffected. Moreover, in the present stroke population, lesions are very small. For each patient, the structural MRI images underwent a procedure of a segmentation into gray matter, white matter and cerebrospinal fluid and a normalization onto the Montreal Neurological Institute (MNI) template. CAT uses geodesic shooting registration [24] with predefined templates. Finally, images were smoothed to suppress noise and effects due to residual differences in gyral anatomy, with a kernel of $6 \times 6 \times 6$ mm.

CST integrity

CST integrity was assessed according to the Lam Method [25] that was slightly modified because we thought that it was more pertinent to calculate an area of interrupted CST fibers instead of a volume. We chose the meanT1 axial slice perpendicular to the CST tract that showed the maximal overlap, as shown in Fig. 1. The percentage of CST lesion was calculated from the area of intersection between the lesion area and the CST area.

Statistical analyses

DTI

Statistical analyses were performed using GraphPad Prism, and mean and SD were calculated. The threshold for statistical significance was set to p value < 0.05 . The ratio of FA (FA_r) was calculated by dividing the ipsilesional to the contralesional values. We first assessed the correlation between FA_r on the three different ROIs and the motor tests at follow-up (approximately 4 months), using a linear regression model. To further probe the relationship between motor skill and microstructural status of white matter tracts, we classified patients in subgroups with mild or moderate deficit (threshold 30 s for the NPHT and 30 kg for the DYN) [26–28] and compared their FA using the parametric statistics, after checking that our data followed a normal law (with a Shapiro–Wilk test).

Alternative motor fibers: To assess the impact of aMF on clinical recovery, we initially separated patients into two groups. The first group was those from whom the tractography method found alternative pathways, either passing via the corpus callosum or via the rubro- and/or reticulospinal pathways and whatever the delay (baseline or follow-up). The second group that did not display alternative fibers,

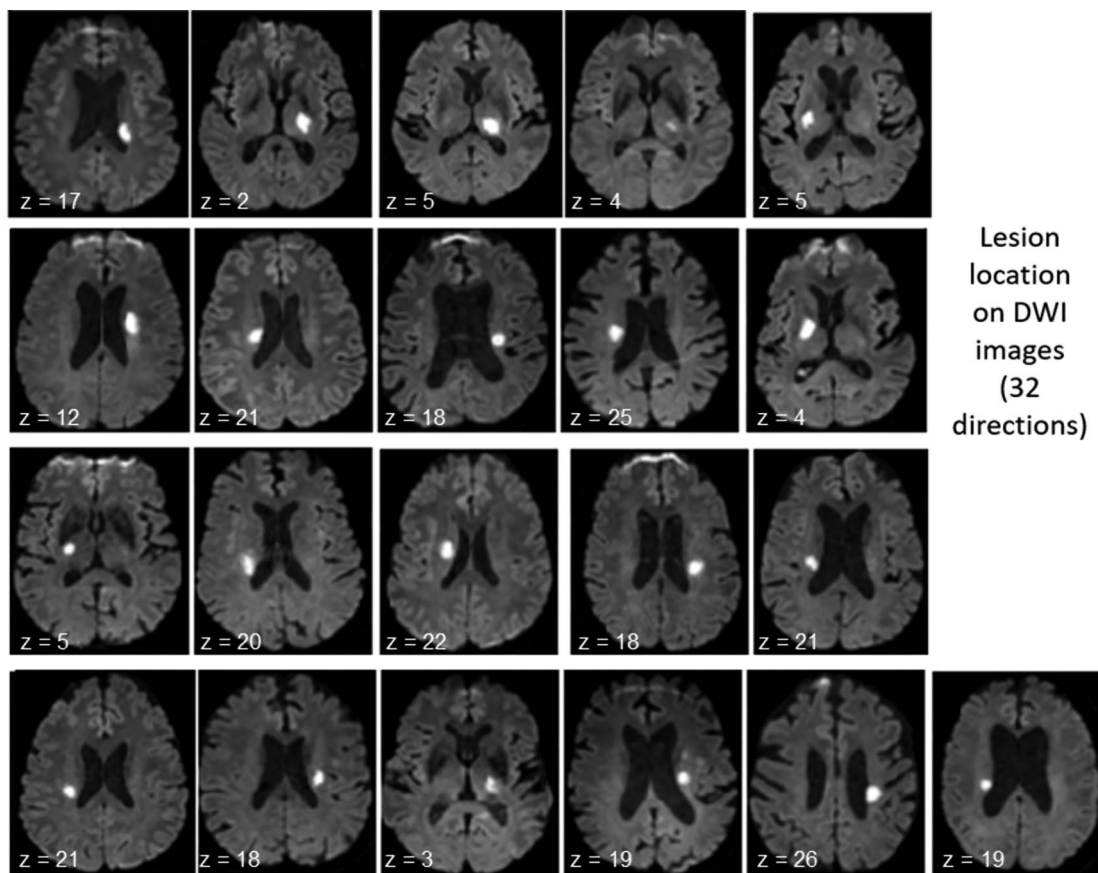


Fig. 1 Lesion location on DWI images at baseline ($n=21$ patients). z in mm above AC–PC plane

neither at baseline nor at follow-up. For each of these two groups, we calculated and compared the average clinical scores for the different tests at baseline and follow-up. We also calculated if there was a correlation between the presence of alternative motor fibers (aMF) and the progression of the recovery, i.e., difference between the score at follow-up and at baseline. Finally, we wanted to verify the impact of the presence of rubro- and/or reticulospinal pathways found by tractography at follow-up on motor recovery.

VBM

For longitudinal analysis using the SPM12 software, parametric tests were performed. We performed two analyses: first, whether there were any significant gray matter volume (GMV) changes across time, at baseline and follow-up for the whole patient cohort. For this analysis, a general univariate linear model and paired T-test was used under SPM12 to generate a statistical map comparing the baseline and follow-up T1 images. TIV (total intracranial volume) and age were included as covariates. When including age as covariate, no effect of age was found on the results. The threshold of significance set was $p \leq 0.001$, cluster-level correction:

clusters ≥ 100 voxels were considered as significant. The second analyses tested whether there were significant linear correlations between GMV and motor recovery scores. These second analyses were implemented as a simple regression model, with the GMV changes maps as a dependent variable, and the motor recovery scores as an independent variable ($p < 0.05$).

Results

Demographic and clinical characteristics are shown in Table 1 and Fig. 1. All patients underwent clinical and MRI evaluation at baseline (4.4 days \pm 2.7 from stroke onset) and at follow-up (approximately 4 months after baseline: 111 \pm 22 days after baseline). None patient was lost at follow-up. At inclusion, no patient had an mRS of zero, 10 patients had an mRS of one, 6 had an mRS of two, and 5 had an mRS of four. At follow-up, 5 patients had an mRS of zero, 13 had an mRS of one, and 3 had an mRS of two. All patients improved in mRS, with the exception of one patient whose mRS worsened from 1 to 2. Mean lesional volume was 4.2 \pm 1.9 ml. The NIHSS score was 2.80 \pm 1.47

Table 1 Clinical and demographics characteristics of the 21 patients. Baseline, i.e., at a mean of 4.42 days post-stroke; follow-up: at a mean of 116 days post-stroke

Demographic and clinical characteristics	Patients (n=21)
Age	70 ± 10 [49–87]
Sex (female)	7/21 (33%)
Baseline NIHSS mean; SD; min/max	2.80 ± 1.47 [2–8]
Follow-up NIHSS; mean; SD; min/max	0.26 ± 0.56 [0–2]
NIHSS = 0 at follow-up	79%
mRS at baseline; mean; SD; min/max	2.0 ± 1.22 [1–4]
mRS at follow-up; mean; SD; min/max	0.95 ± 0.52 [0–2]
Lesion location	11
Corona radiata	5
PLIC	2
Corona radiata/PLIC	2
PLIC-thalamus	1
PLIC-putamen-caudate	
Lesion side	11 right/10 left
Mean lesional volume (mL) SD	4.2 ± 1.9
Mean % of damaged CST; SD; min, max	23.3% ± 16.0 [0–57]

at baseline and 0.26 ± 0.56 at follow-up. Spontaneous motor recovery occurred at follow-up and 79% of the patient had a NIHSS score of 0 at follow-up. All patient received standard rehabilitation, which in France corresponds to 45 min-2 h/day for mild-to-moderate impaired patients.

DTI analyses

Supplementary Table 1 shows the evolution of FA for the ipsi- and contralesional CST from the baseline and at follow-up. We calculated the evolution for three different parameters: meanFA for the CST and FA for two ROIs, posterior limb of the internal capsule (PLIC) and corona radiata (CR).

CST

There were no changes in axial, radial or mean diffusivity for the CST (Supplementary Table 2).

MeanFA of the entire CST The ipsilesional meanFA_{CST} was not affected at baseline, whereas it was significantly decreased at follow-up compared to the contralesional side (Supplementary Table 1; Fig. 2).

FA of the posterior limb of the internal capsule At baseline and follow-up, there was a statistical difference between the ipsilesional and contralesional side (Supplementary Table 1; Fig. 2). The ipsilesional FA was significantly lower between baseline and follow-up.

FA of the corona radiata tract At baseline and follow-up, there was statistical difference between the ipsilesional and contralesional sides (Supplementary Table 1, Fig. 2).

Relation to the neurological motor deficit at follow-up

We correlated the FAr at follow-up (approximately 4 months) in the corona radiata ROI and the behavioural tests at follow-up with a regression analysis that showed a trend toward better function associated with a ratio closer to normal (value of one) (Fig. 3A, B, C).

Then, patients were categorized into two subgroups, according to their deficit (mild or moderate) at follow-up and according to previous proposed cutoff [27, 28]. For the NPHT, patients were considered having a moderate deficit if the test was performed in more than 29 s ($n = 9$), and having a mild deficit if the test was performed in less than 30 s ($n = 12$). For the dynamometer, a patient with a score less than 30 kg considered as moderately impaired and over 29 kg was considered as mildly impaired. For each of these two groups, we calculated the average of the FA on each of the 3 regions of interest: posterior limb of the internal capsule, corona radiata and pons (Suppl Table 3). For the NPHT measured at follow-up, the group with most severe initial deficit showed significant decreased FA in posterior limb of internal capsule and corona radiata (Suppl Table 3). For the dynamometer at follow-up, there was a significant group effect but post hoc analyses were not significant due to the low sample size in one group.

We calculated the percentage of CST lesion to assess CST integrity. We did not find any correlation, suggesting that CST integrity was not the only factor explaining motor deficit.

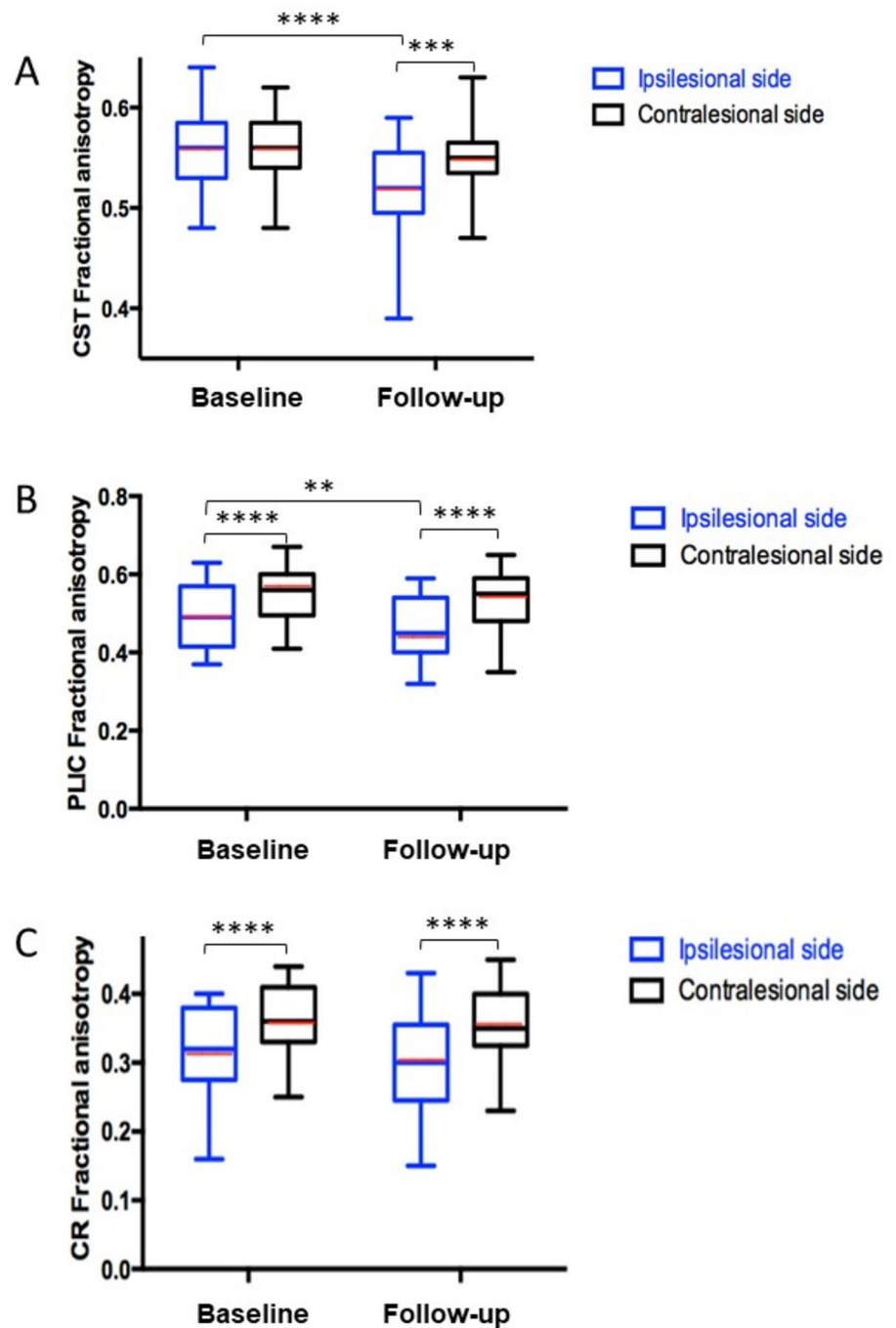
Alternative pathways

There is no statistically significant difference on the motor measures at any time between the two groups (aMF and no aMF) whatever the delay and whatever the test (Suppl Table 4).

VBM analyses

Voxel-wise paired t-tests on the gray matter (GM) between the acute and subacute stages of stroke demonstrated significant increase in GM in the ipsilesional premotor cortex, hippocampus and fornix, lingual gyrus and cingular anterior cortex (Fig. 4; Table 2). No decrease in GM suggesting atrophy was evidenced.

Fig. 2 FA results. Graph of the evolution of mean FA between ipsi- and contralesional sides from the acute to the subacute stages for the entire CST (A), the PLIC (B), and the CR (C). Median, mean (red line), first and third quartiles, minima and maxima. *: $p < 0.05$; **: $p < 0.005$; ***: $p < 0.001$; ****: $p < 0.0001$



Correlations between the changes in GM and the clinical variables

GMV changes and the changes in the motor measures between follow-up and baseline were positively correlated in the anterior cingulum for the NPHT, HTT and DYN (Fig. 5A, B, C, $p < 0.05$, corrected).

Discussion

As far as we know, this is the first human study looking at both DTI and VBM changes longitudinally and in a very selected population of stroke patients with pure motor deficits.

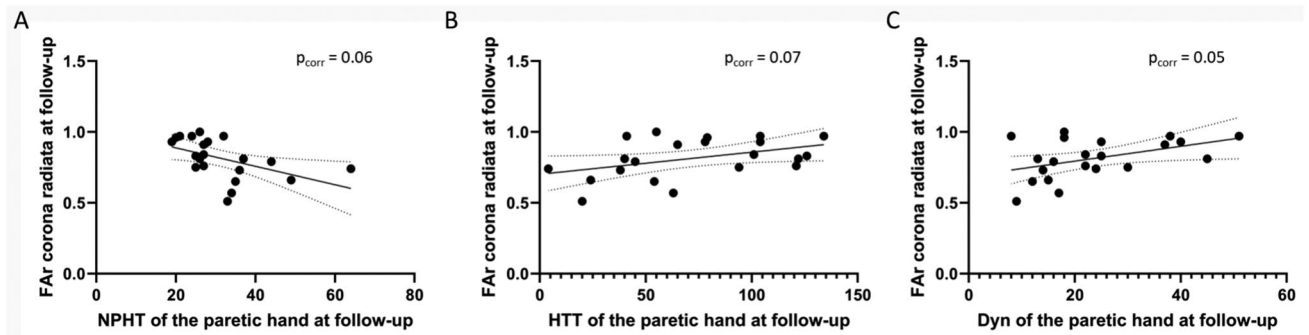


Fig. 3 Correlation between MRI DTI parameters and motor test scores. Correlation of the FAR (ratio ipsi/contralateral FA) at follow-up in the ROI corona radiata and scores at the NPHT (A), HTT (B), and DYN (C) for the paretic side at follow-up. Pearson test corrected

for multiple comparisons (Bonferroni–Holm correction) [29], respectively, $p=0.06$, $r^2=0.25$, $p=0.07$, $r^2=0.18$, $p=0.05$, $r^2=0.20$; 95% confidence interval

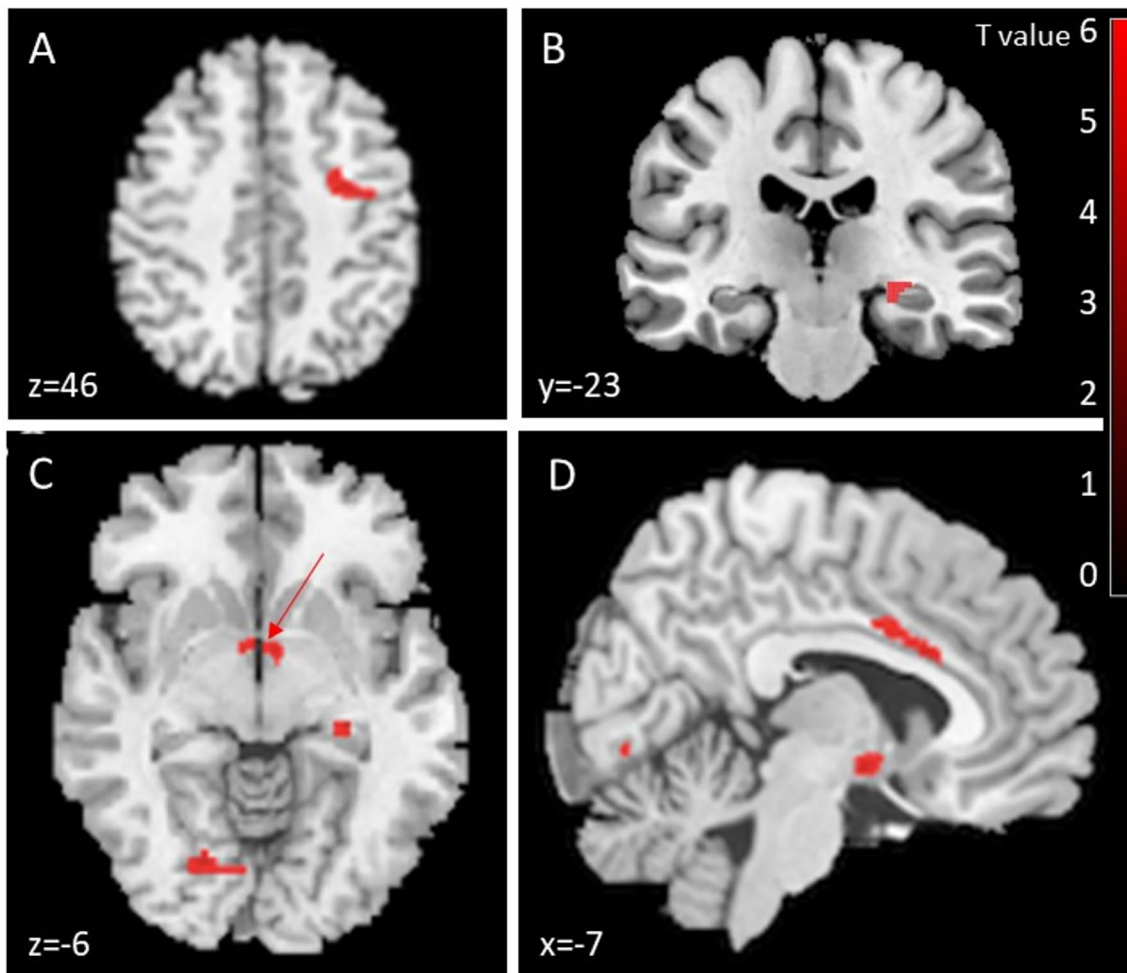


Fig. 4 VBM results. VBM MRI axial, coronal and sagittal slices showing in red increased GM in the premotor cortex (A), the ipsilateral hippocampus (B), bilateral fornix (red arrow), lingual gyrus

(C) and cingulate anterior cortex (D) between baseline and follow-up ($p \leq 0.001$, cluster-level correction: clusters ≥ 100 voxels)

Table 2 Brain regions exhibiting increased GM at follow-up (approximately 4 months) ($p < 0.001$). MNI: Montreal Neurological Institute

Brain region	MNI coordinates of maximum (X, Y, Z)	Cluster size (voxels)
Increased gray matter		
Ipsilesional premotor cortex	(42; -4.5; 42)	337
Ipsilesional hippocampus	(27; -25.5; -7.5)	179
Bilateral fornix	(-3; -3; -1)	
Lingual gyrus	(-19.5; -73.5; 6)	162
Cingular anterior cortex	(-6; 6; 31.5)	125

For the evolution of FA, we compared ipsi- and contralateral CST at the acute and subacute phase post-stroke. The DTI analysis was focused on the CST originating in the primary motor cortex. In the acute phase (first 10 days), there was no difference between ipsi- and contralateral CST. This result is consistent to previous studies [7, 8, 16–19, 25, 30–32]. Puig et al. found absolute and relative FA decreases at 30 days after stroke, but not at 12 h or 3 days after stroke [7], whereas Doughty et al. found a subtle but significant changes in FA in cerebral peduncles, however, with larger lesions [8].

However, when we calculate the FA in a ROI involving the lesion (e.g., posterior limb of internal capsule) or above (corona radiata), in the acute phase, FA was statistically lower in the affected side, meaning that the Wallerian degeneration had started but only around the lesion. This change was detectable despite small lesions. At follow-up, the FA was statistically lower in the ipsilesional than in the contralateral CST, because retrograde Wallerian degeneration had occurred along the pyramidal tract. We showed a significant correlation between FA and motor function of the affected side (NPHT, HTT, and DYN) and could classify patients according to the severity of the deficit.

FA values represent the degree of directionality of microstructures (e.g., axons, myelin and microtubules). Reduced FA values appear to be related to the disintegration of fibers and Wallerian degeneration. These results are in agreement with the previous studies that evaluate the relationship between the CST status and motor function in stroke patients [33]. We found that the FA of CST accounts for 18–25% of the variability of the motor status, which is relatively lower than previous reports. One of the reasons is that, at follow-up, most patients have recovered well and homogeneously (Table 1). It, therefore, appears more difficult to establish correlations.

Alternate motor fibers (aMF) which includes reticulo-, rubrospinal pathways and transcallosal fibers may also be important for recovery [10, 13, 34]. However, their post-stroke role, benefit or harmful, is not fully understood, and may vary, depending on the post-stroke stage [35]. In DTI studies, it seems that the presence of aMF in the chronic post-stroke phase is beneficial [30]. Nevertheless, there is no longitudinal DTI studies that evaluate the evolution of aMF during acute and subacute stages of stroke and their impact on clinical recovery.

In our study, we did not find any correlations between the probabilistic presence of alternate motor fibers detected by tractography and motor recovery, whatever the post-stroke stage (acute or subacute). Among this group of patients recovering well, it could demonstrate different plasticity processes, proving effective individual recovery strategies. Lindenberg et al. [30] in a 35 chronic stroke patient study found poor recovery when both tracts (CST and aMF) were affected, but moderate or better recovery when the aMF tract was unaffected. Karbasforoushan et al. measured the FA of CST and alternate motor tracts in the spine and found that motor recovery relied on the contralateral medial reticulospinal tract in severely impaired patients [36]. However, our study shows a small

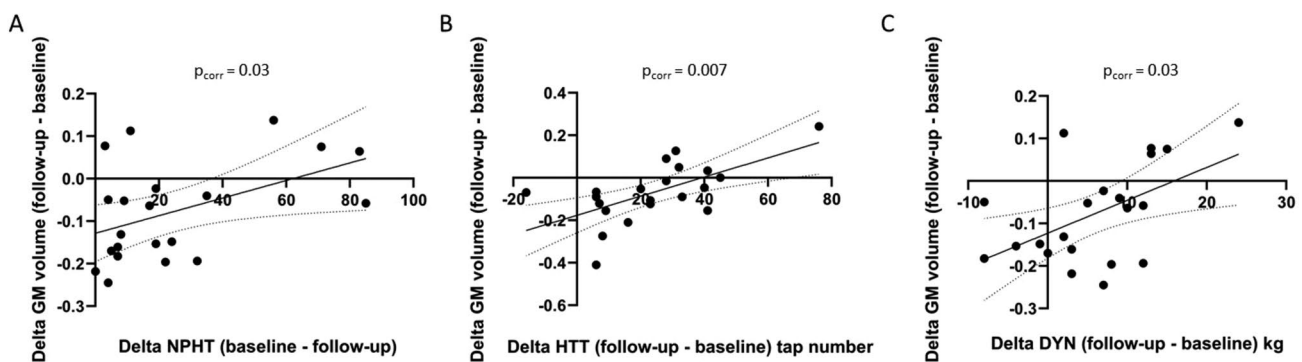


Fig. 5 Correlation between MRI VBM parameters and motor score changes. Correlation between the change in gray matter volume in the contralateral anterior cingulum and the improvement at the NPHT (A), HTT (B), and DYN (C) between baseline and follow-up.

(Pearson test corrected for multiple comparisons, $p = 0.03$, $r^2 = 0.22$, $p = 0.007$, $r^2 = 0.39$; $p = 0.03$, $r^2 = 0.27$; 95% confidence interval; $x = -9$; $y = 21$; $z = 27$)

or punctual involvement of alternate motor tracts in mildly impaired patients.

With VBM, we found significant increased GM volumes in areas distant from the primary lesion site between the acute and subacute stages post-stroke. Four sites presented increased cortical thickness at follow-up. The ipsilesional premotor cortex was the larger location. It corresponds to Brodmann's area 6, which is directly connected to infarcted areas in the present study. Indeed, the premotor cortex emits 20% of the fibers constituting the CST and also sends efferences to the primary motor cortex. The upper limb is represented by a larger number of neurons than in the primary motor cortex [37]. Abela et al. [38], in a prospective study of 28 patients, also found increased cortical thickness of the premotor ipsilesional cortex at 3 and 9 months post-infarction. No effects related to the injured hemisphere were found in the regions described in the present VBM study in subcortical patients [39]. Thus, the flipping procedure we applied does not challenge our results.

We can wonder what is the link between DTI and VBM changes and whether the Wallerian degeneration of the CST has a consequence on the increased GM in the ipsilesional premotor cortex. However, no correlation was found. It can be hypothesized that this increased cortical thickness of the ipsilesional premotor cortex reflects both restorative and compensatory phenomena for the hand involving i. redundancy of the hand representation and more involvement of CST premotor fibers and II. maybe a vicariance process with the take of a new role of premotor neurons in driving motor command [40].

As for the hippocampus, it is consistent with different previous studies. Fan et al. in 10 patients had also found increased cortical thickness of the hippocampus that correlated with clinical recovery [41]. Yu et al. found increased cortical thickness of the hippocampus at 6 months in 12 patients [42]. Finally, Gauthier emphasized the contribution of the structural plasticity of the hippocampus to the therapy-induced recovery of motor function in stroke patients after constraint-induced movement therapy [43]. An increased cortical thickness of fornix fibers connecting the mammillary bodies to the hippocampus is in agreement with these results. Eriksson et al., in 1998 [44], showed that human hippocampus retains its ability to generate neurons throughout life. Jin et al. showed that there were small capacities of neurogenesis in the periventricular zone and hippocampus post-stroke [45]. We can wonder if the recruitment of cognitive resources is beneficial on motor recovery. This hippocampal increased cortical thickness was not associated with an improvement in cognitive performance nor in mnemonic capacities since the patients were not impaired but may be due to a relearning of the motor functions.

The lingual gyrus has a role in the visual perception of movement. Visual analysis of the movement of the healthy

limb could allow recovery and thus lead to increased cortical thickness of the lingual gyrus. Two studies also found increased cortical thickness of this gyrus [41, 42]. The two latter localizations suggest that non-motor function such as cognition and vision are recruited to facilitate motor recovery after stroke since 'spatiality' is an important feature of movements.

The anterior cingulate cortex has direct motor connections to the different cortical regions involved in motor control: the premotor cortex and the supplementary motor area. It corresponds to Brodmann area 24. This increased cortical thickness would, therefore, correspond to an adaptive plasticity and a direct compensating motor phenomenon since it was correlated to improved recovery.

In the present longitudinal MRI study, even if lesions were relatively small, some cortical brain regions showed significant changes in volume sometimes with a statistical correlation with motor recovery. This reorganization would, therefore, be a restorative phenomenon. The hypothesis underlying cortical thickness modifications are derived from pre-clinical histological studies in rats [40, 46–51]. Increased cortical thickness is possibly linked to a neurogenesis. It could also be a dendritic sprouting or synaptogenesis. Neurogenesis abilities have been described by Eriksson and Jin in post-stroke patients [44, 45].

Our study has some limitations: it applies only to patients having a mild or moderate deficit and a good recovery at 4 months making difficult to establish correlations between clinical outcomes and microstructural modifications. However, we found a correlation with the anterior cingulum. The group was homogeneous with good recovery and only 23.3% loss of CST fibers suggesting that enough direct fibers and minor reorganization can sustain recovery without the intervention of alternate motor fibers (40). Another limitation was that we explore the CST emanating from M1 only and did not examine the part originating from the premotor cortex. However, since we show that in this group of patients with very small lesions, reorganization takes place in the premotor cortex, pulling the latter with the primary cortex could have put together opposite changes, degenerating and regenerating processes. The strengths of our study are a longitudinal follow-up at two different time points post-stroke (acute and subacute) and a homogeneous group recruited on a pure motor deficit.

Conclusion

In the present study, we confirmed that motor outcome is highly dependent on lesion location and particularly on CST microstructural status. We were able to identify post-stroke adaptive processes with two different neuroimaging techniques that showed complementary results. DTI

tractography demonstrated substantial Wallerian degeneration, and suggested the presence of alternative circuits in some patients via the corpus callosum or the rubro- and reticulospinal pathways, which were not evidenced, however, to be associated with motor recovery in this study. This comforted us to interpret the VBM increased cortical thickness of the premotor cortex, anterior cingulum and hippocampus as substrate of a successful strategy of recovery, mainly implicating premotor CST fibers. Indeed, DTI and VBM give potential predictive biomarkers of post-stroke recovery. They make it possible to evaluate both the anatomical and functional reorganization. A better knowledge of the mechanisms of brain plasticity may lead to more precise therapeutic interventions.

Supplementary Information The online version contains supplementary material available at <https://doi.org/10.1007/s00415-024-12648-y>.

Acknowledgements We thank the Inserm/UPS UMR1214 Technical Platform for their help in setting up and for the acquisitions of the MRI sequences. We also thank Charlotte Rosso for sharing the reticulospinal tract template.

Author contributions FC: supervision, study conceptualization (lead), funding acquisition, data interpretation and validation; JR, ML, IL: bibliographic work, investigation, formal analysis and interpretation of the data, statistics, writing, original draft preparation. IL: VBM validation, writing: review and editing. JR, ML, MP: project administration, investigation and data curation. NC: statistics and figure artwork.

Funding Open access funding provided by Université Toulouse III - Paul Sabatier. The study was supported by a grant from the Toulouse Purpan Hospital.

Data availability The data that support the findings of this study are available from the corresponding author upon reasonable request.

Declarations

Conflict of interest The authors have no conflict of interest to disclose.

Open Access This article is licensed under a Creative Commons Attribution 4.0 International License, which permits use, sharing, adaptation, distribution and reproduction in any medium or format, as long as you give appropriate credit to the original author(s) and the source, provide a link to the Creative Commons licence, and indicate if changes were made. The images or other third party material in this article are included in the article's Creative Commons licence, unless indicated otherwise in a credit line to the material. If material is not included in the article's Creative Commons licence and your intended use is not permitted by statutory regulation or exceeds the permitted use, you will need to obtain permission directly from the copyright holder. To view a copy of this licence, visit <http://creativecommons.org/licenses/by/4.0/>.

Bibliography

- Goyal M, Menon BK, Van Zwam WH, Dippel DWJ, Mitchell PJ, Demchuk AM et al (2016) Endovascular thrombectomy after large-vessel ischaemic stroke: a meta-analysis of individual patient data from five randomised trials. *Lancet* 387(10029):1723–1731. [https://doi.org/10.1016/S0140-6736\(16\)00163-X](https://doi.org/10.1016/S0140-6736(16)00163-X)
- Go AS, Mozaffarian D, Roger VL, Benjamin EJ, Berry JD, Borden WB et al (2013) Heart disease and stroke statistics–2013 update: A report from the American Heart Association. *Circulation*. [https://doi.org/10.1016/S0140-6736\(16\)00163-X](https://doi.org/10.1016/S0140-6736(16)00163-X)
- Kwakkel G, Lannin NA, Borschmann K, English C, Ali M, Churilov L et al (2017) Standardized measurement of sensorimotor recovery in stroke trials: consensus-based core recommendations from the stroke recovery and rehabilitation roundtable. *Int J Stroke* 12(125):451–461. <https://doi.org/10.1177/1747493017711813>
- Pierpaoli C, Barnett A, Pajevic S, Chen R, Penix LR, Virta A, et al. Water diffusion changes in Wallerian degeneration and their dependence on white matter architecture. *Neuroimage* [Internet]. 2001;13(6 Pt 1):1174–85. <http://www.sciencedirect.com/science/article/pii/S1053811901907657>
- Schaechter JD, Fricker ZP, Perdue KL, Helmer KG, Vangel MG, Greve DN et al (2009) Microstructural status of ipsilesional and contralesional corticospinal tract correlates with motor skill in chronic stroke patients. *Hum Brain Mapp* 30(11):3461–3474. <https://doi.org/10.1002/hbm.20770>
- Stinear CM, Barber PA, Smale PR, Coxon JP, Fleming MK, Byblow WD (2007) Functional potential in chronic stroke patients depends on corticospinal tract integrity. *Brain* 130(1):170–180. <https://doi.org/10.1093/brain/awl333>
- Puig J, Blasco G, Daunis-I-Estadella J, Thomalla G, Castellanos M, Figueras J et al (2013) Decreased corticospinal tract fractional anisotropy predicts long-term motor outcome after stroke. *Stroke* 44(7):2016–2018. <https://doi.org/10.1161/STROKEAHA.111.000382>
- Doughty C, Wang J, Feng W, Hackney D, Pani E, Schlaug G (2016) Detection and predictive value of fractional anisotropy changes of the corticospinal tract in the acute phase of a stroke. *Stroke* 47(6):1520–1526. <https://doi.org/10.1161/STROKEAHA.115.012088>
- Lin LY, Ramsey L, Metcalf NV, Rengachary J, Shulman GL, Shimony JS et al (2018) Stronger prediction of motor recovery and outcome post-stroke by cortico-spinal tract integrity than functional connectivity. *PLoS One* [Internet]. 13(8):1–13. <https://doi.org/10.1371/journal.pone.0202504>
- Schulz R, Park E, Lee J, Chang WH, Lee A, Kim YH et al (2017) Synergistic but independent: the role of corticospinal and alternate motor fibers for residual motor output after stroke. *NeuroImage Clin* 15:118–124. <https://doi.org/10.1016/j.nicl.2017.04.016>
- Schulz R, Park E, Lee J, Chang WH, Lee A, Kim YH et al (2017) Interactions between the corticospinal tract and premotor-motor pathways for residual motor output after stroke. *Stroke* 48(10):2805–2811. <https://doi.org/10.1161/STROKEAHA.117.01683>
- Schulz R, Runge CG, Bönstrup M, Cheng B, Gerloff C, Thomalla G et al (2019) Prefrontal-premotor pathways and motor output in well-recovered stroke patients. *Front Neurol* 10:105. <https://doi.org/10.3389/fneur.2019.00105>
- Jang SH, Lee SJ (2019) Corticoreticular tract in the human brain: a mini review. *Front Neurol* 10(November):1–9. <https://doi.org/10.3389/fneur.2019.01188>
- Moulton E, Valabregue R, Lehericy S, Samson Y, Rosso C (2019) Multivariate prediction of functional outcome using lesion topography characterized by acute diffusion tensor imaging. *NeuroImage Clin Internet* 23:101821. <https://doi.org/10.1016/j.nicl.2019.101821>
- Ashburner J, Friston KJ (2000) Voxel-based morphometry - The methods. *Neuroimage* 11:805–821. <https://doi.org/10.1006/nimg.2000.0582>
- Dang C, Liu G, Xing S, Xie C, Peng K, Li C et al (2013) Longitudinal cortical volume changes correlate with motor

- recovery in patients after acute local subcortical infarction. *Stroke* 44(10):2795–2801. <https://doi.org/10.1161/STROKEAHA.113.000971>
17. Yin D, Yan X, Fan M, Hu Y, Men W, Sun L et al (2013) Secondary degeneration detected by combining voxel-based morphometry and tract-based spatial statistics in subcortical strokes with different outcomes in hand function. *Am J Neuroradiol* [Internet]. 34(7):1341–7
 18. Yang M, Yang YR, Li HJ, Lu XS, Shi YM, Liu B et al (2015) Combining diffusion tensor imaging and gray matter volumetry to investigate motor functioning in chronic stroke. *PLoS ONE* 10(5):e0125038. <https://doi.org/10.1371/journal.pone.0125038>
 19. Nakashima A, Moriuchi T, Mitsunaga W, Yonezawa T, Kataoka H, Nakashima R et al (2017) Prediction of prognosis of upper-extremity function following stroke-related paralysis using brain imaging. *J Phys Ther Sci* 29(8):1438–1443. <https://doi.org/10.1589/jpts.29.1438>
 20. Huppertz HJ, Kröll-Seger J, Klöppel S, Ganz RE, Kassubek J (2010) Intra- and interscanner variability of automated voxel-based volumetry based on a 3D probabilistic atlas of human cerebral structures. *Neuroimage* [Internet]. 49(3):2216–2224. <https://doi.org/10.1016/j.neuroimage.2009.10.066>
 21. Yeh F-C, Panesar S, Fernandes D, Meola A, Yoshino M, Fernandez-Miranda JC et al (2017) Population-Averaged Atlas Of The Macroscale Human Structural Connectome and its network topology. *NeuroImage* 2018(178):57–68. <https://doi.org/10.1016/j.neuroimage.2018.05.027>
 22. Rorden C, Brett M (2000) Stereotaxic display of brain lesions. *Behav Neurol* 12(4):191–200. <https://doi.org/10.1155/2000/421719>
 23. Brett M, Leff AP, Rorden C, Ashburner J (2001) Spatial normalization of brain images with focal lesions using cost function masking. *Neuroimage* 14(2):486–500. <https://doi.org/10.1006/nimg.2001.0845>
 24. Ashburner J, Friston KJ (2011) Diffeomorphic registration using geodesic shooting and Gauss-Newton optimisation. *Neuroimage* 55(3–3):954–967. <https://doi.org/10.1016/j.neuroimage.2010.12.049>
 25. Lam TK, Binns MA, Honjo K, Dawson DR, Ross B, Stuss DT et al (2018) Variability in stroke motor outcome is explained by structural and functional integrity of the motor system. *Sci Rep* 8(1):9480. <https://doi.org/10.1038/s41598-018-27541-8>
 26. Feys H, De Weerd W, Verbeke G, Steck GC, Capiou C, Kiekens C et al (2004) Early and repetitive stimulation of the arm can substantially improve the long-term outcome after stroke: a 5-year follow-up study of a randomized trial. *Stroke* 35(4):924–929. <https://doi.org/10.1161/01.STR.0000121645.44752.f7>
 27. Feys P, Lamers I, Francis G, Benedict R, Phillips G, LaRocca N et al (2017) The nine-hole peg test as a manual dexterity performance measure for multiple sclerosis. *Mult Scler* 23(5):711–720. <https://doi.org/10.1177/1352458517690824>
 28. Stuck AK, Mäder NC, Bertschi D, Limacher A, Kressig RW (2021) Performance of the ewgsop2 cut-points of low grip strength for identifying sarcopenia and frailty phenotype: a cross-sectional study in older inpatients. *Int J Environ Res Public Health* 18(7):3498. <https://doi.org/10.3390/ijerph18073498>
 29. Sankoh AJ, Huque MF, Dubey SD (1997) Some comments on frequently used multiple endpoint adjustment methods in clinical trials. *Stat Med*. 16(22):2529–2542
 30. Lindenberger R, Renga V, Zhu LL, Betzler F, Alsop D, Schlaug G (2010) Structural integrity of corticospinal motor fibers predicts motor impairment in chronic stroke. *Neurology* 74(4):280–287. <https://doi.org/10.1212/WNL.0b013e3181cccc6d9>
 31. Bashir S, Kaeser M, Wyss A, Hamadjida A, Liu Y, Bloch J et al (2012) Short-term effects of unilateral lesion of the primary motor cortex (M1) on ipsilesional hand dexterity in adult macaque monkeys. *Brain Struct Funct* 217(1):63–79. <https://doi.org/10.1007/s00429-011-0327-8>
 32. Liu X, Tian W, Li L, Kolar B, Qiu X, Chen F et al (2012) Hyperintensity on diffusion weighted image along ipsilateral cortical spinal tract after cerebral ischemic stroke: a diffusion tensor analysis. *Eur J Radiol* [Internet]. 81(2):292–297. <https://doi.org/10.1016/j.ejrad.2010.12.053>
 33. Thomalla G, Glauche V, Koch MA, Beaulieu C, Weiller C, Röther J (2004) Diffusion tensor imaging detects early Wallerian degeneration of the pyramidal tract after ischemic stroke. *Neuroimage* 22(4):1767–1774. <https://doi.org/10.1016/j.neuroimage.2004.03.041>
 34. Soulard J, Huber C, Baillieux S, Thuriot A, Renard F, Broche BA et al (2020) Motor tract integrity predicts walking recovery: a diffusion MRI study in subacute stroke. *Neurology* 94(6):E583–E593. <https://doi.org/10.1212/WNL.00000000000008755>
 35. Ward NS (2006) The neural substrates of motor recovery after focal damage to the central nervous system. *Arch Phys Med Rehabil* 87(12 SUPPL.):30–35. <https://doi.org/10.1016/j.apmr.2006.08.334>
 36. Karbasforoushan H, Cohen-Adad J, Dewald JPA (2019) Brainstem and spinal cord MRI identifies altered sensorimotor pathways post-stroke. *Nat Commun* 10(1):1–7. <https://doi.org/10.1038/s41467-019-11244-3>
 37. Dum RP, Strick PL (1991) The origin of corticospinal projections from the premotor areas in the frontal lobe. *J Neurosci* 11(March):667–689. <https://doi.org/10.1523/JNEUROSCI.11-03-00667.1991>
 38. Abela E, Seiler A, Missimer JH, Federspiel A, Hess CW, Sturzenegger M et al (2015) Grey matter volumetric changes related to recovery from hand paresis after cortical sensorimotor stroke. *Brain Struct Funct* [Internet]. 220(5):2533–2550. <https://doi.org/10.1007/s00429-014-0804-y>
 39. Diao Q, Liu J, Wang C, Cao C, Guo J, Han T et al (2017) Gray matter volume changes in chronic subcortical stroke: a cross-sectional study. *NeuroImage Clin* [Internet]. 14:679–684. <https://doi.org/10.1016/j.nicl.2017.01.031>
 40. Cirillo C, Brihmat N, Castel-Lacanal E, Le Fricc A, Barbieux-Guillot M, Raposo N et al (2020) Post-stroke remodeling processes in animal models and humans. *J Cereb Blood Flow Metab* 40(1):3–22. <https://doi.org/10.1177/0271678X19882788>
 41. Fan F, Zhu C, Chen H, Qin W, Ji X, Wang L et al (2013) Dynamic brain structural changes after left hemisphere subcortical stroke. *Hum Brain Mapp* 34:1872–1881. <https://doi.org/10.1002/hbm.22034>
 42. Yu X, Yang L, Song R, Jiaerken Y, Yang J, Lou M et al (2017) Changes in structure and perfusion of grey matter tissues during recovery from Ischaemic subcortical stroke: a longitudinal MRI study. *Eur J Neurosci* 46(7):2308–2314. <https://doi.org/10.1111/ejn.13669>
 43. Gauthier LV, Taub E, Perkins C, Ortmann M, Mark VW, Uswatte G (2008) Remodeling the brain plastic structural brain changes produced by different motor therapies after stroke. *Stroke* 39(5):1520–1525. <https://doi.org/10.1161/STROKEAHA.107.502229>
 44. Eriksson PS, Perfilieva E, Björk-Eriksson T, Alborn A-M, Nordborg C, Peterson DA et al (1998) Neurogenesis in the adult human hippocampus. *Nat Med* 4(11):1313–1317. <https://doi.org/10.1038/3305>
 45. Jin K, Wang X, Xie L, Mao XO, Zhu W, Wang Y, et al. Evidence for stroke-induced neurogenesis in the human brain. *Proc Natl Acad Sci U S A* [Internet]. 2006;103(35):13198–202. <http://www.ncbi.nlm.nih.gov/pubmed/16924107%5Cn>, <http://www.pubmedcentral.nih.gov/articlerender.fcgi?artid=PMC1559776>

46. Carmichael ST (2006) Cellular and molecular mechanisms of neural repair after stroke: making waves. *Ann Neurol* 59(5):735–742. <https://doi.org/10.1002/ana.20845>
47. Joy MT, Carmichael ST (2021) Encouraging an excitable brain state: mechanisms of brain repair in stroke. *Nat Rev Neurosci* [Internet]. 22(1):38–53. <https://doi.org/10.1038/s41583-020-00396-7>
48. Carmichael ST, Kathirvelu B, Schweppe CA, Nie EH (2017) Molecular, cellular and functional events in axonal sprouting after stroke. *Exp Neurol* [Internet]. 287:384–394. <https://doi.org/10.1016/j.expneurol.2016.02.007>
49. Colitti N, Desmoulin F, Le Friec A, Labriji W, Robert L, Michaux A et al (2022) Long-term intranasal nerve growth factor treatment favors neuron formation in de novo brain tissue. *Front Cell Neurosci* 16:871532. <https://doi.org/10.3389/fncel.2022.871532>
50. Le Friec A, Salabert AS, Davoust C, Demain B, Vieu C, Vaysse L et al (2017) Enhancing plasticity of the central nervous system: drugs, stem cell therapy, and neuro-implants. *Neural Plast* 12:98–111. <https://doi.org/10.1155/2017/2545736>
51. Loubinoux I, Brihmat N, Castel-Lacanal E, Marque P (2017) Cerebral imaging of post-stroke plasticity and tissue repair. *Rev Neurol (Paris)* 173(9):577–583. <https://doi.org/10.1016/j.neurol.2017.09.007>